HHS Public Access

Author manuscript

Brain Struct Funct. Author manuscript; available in PMC 2018 July 11.

Published in final edited form as:

Brain Struct Funct. 2017 January ; 222(1): 267–285. doi:10.1007/s00429-016-1215-z.

Meta-analytic connectivity modeling of the human superior temporal sulcus

Laura C. Erickson[1,2], **Josef P. Rauschecker**[2,3], and **Peter E. Turkeltaub**[1,4]

[1]Neurology Department, Georgetown University Medical Center, 4000 Reservoir Road NW, Building D, Suite 165, Washington DC, 20057

[2]Neuroscience Department, Georgetown University Medical Center, 3900 Reservoir Road NW, New Research Building, Room WP19, Washington DC, 20057

[3]Institute for Advanced Study, Technische Universität München Lichtenbergstraße 2, 85748 Garching bei München, Germany

[4]Research Division, MedStar National Rehabilitation Hospital 102 Irving St NW, Washington DC, 20010

Abstract

The superior temporal sulcus (STS) is a critical region for multiple neural processes in the human brain (Hein and Knight 2008). To better understand the multiple functions of the STS it would be useful to know more about its consistent functional coactivations with other brain regions. We used the meta-analytic connectivity modeling (MACM) technique to determine consistent functional coactivation patterns across experiments and behaviors associated with bilateral anterior, middle, and posterior anatomical STS subregions. Based on prevailing models for the cortical organization of audition and language, we broadly hypothesized that across various behaviors the posterior STS (pSTS) would coactivate with dorsal-stream regions, whereas the anterior STS (aSTS) would coactivate with ventral-stream regions. The results revealed distinct coactivation patterns for each STS subregion, with some overlap in the frontal and temporal areas, and generally similar coactivation patterns for the left and right STS. Quantitative comparison of STS subregion coactivation maps demonstrated that the pSTS coactivated more strongly than other STS subregions in the same hemisphere with dorsal-stream regions, such as the inferior parietal lobule (only left pSTS), homotopic pSTS, precentral gyrus and supplementary motor area. In contrast, the aSTS showed more coactivation with some ventral-stream regions, such as the homotopic anterior temporal cortex and left inferior frontal gyrus, pars orbitalis (only right aSTS). These findings demonstrate consistent coactivation maps across experiments and behaviors for different anatomical STS subregions, which may help future studies consider various STS functions in the broader context of generalized coactivations for individuals with and without neurological disorders.

Corresponding Author: Peter E. Turkeltaub, 4000 Reservoir Road NW, Building D, Suite 165, Washington DC, 20057, turkeltp@georgetown.edu, 202-784-1764.

Conflict of Interest: The authors declare that they have no conflict of interest.

This article does not contain any studies with human participants or animals performed by any of the authors.

Keywords

superior temporal sulcus; coactivation; meta-analytic connectivity modeling; connectivity; network; dorsal stream

Introduction

The superior temporal sulcus (STS) is a critical association area of the brain that has been implicated in numerous neural processes (Allison et al. 2000; Hein and Knight 2008; Beauchamp 2011), and neurological disorders, e.g., autism spectrum disorders (Redcay 2008; Shih et al. 2011; Zilbovicius et al. 2006). The overlap of different functions in the STS makes it an interesting and complex brain region to study. Differential network coactivations for various functions (Hein and Knight 2008) as well as convergence of multisensory processes (Beauchamp 2015) have both been suggested to support aspects of STS multi-functionality. However, how the STS processes multiple functions is still not well understood. A comprehensive examination of general STS connectivity, coactivation and network associations across functions may be useful to help clarify STS organization and processing capabilities.

In the literature, STS connectivity hypotheses have been incorporated into neuroanatomical network models of various perceptual and cognitive domains (Rauschecker and Tian 2000; Giese and Poggio 2003; Hickok and Poeppel 2007; Rauschecker and Scott 2009; Bornkessel-Schlesewsky et al. 2015; Bernstein and Liebenthal 2014; Allison et al. 2000; Haxby et al. 2000; Iacoboni 2005; Iacoboni and Dapretto 2006; Driver and Noesselt 2008; van Atteveldt et al. 2009; Beauchamp et al. 2004). However, these neural processes are often considered in isolation (Hein and Knight 2008), making it unclear how STS connectivity can be generalized across various functional processes. Previous connectivity studies have only assessed a portion of the STS (Buchsbaum et al. 2005; Nath and Beauchamp 2011; Bishop and Miller 2009; Turk-Browne et al. 2010; Noesselt et al. 2007; Powers et al. 2012; Sokolov et al. 2014; Simmons and Martin 2012; Turken and Dronkers 2011) or reported STS connectivity during the investigation of another area (Zhang et al. 2009; Beer et al. 2011; Margulies and Petrides 2013; Deen et al. 2011). While some studies have assessed resting, task-related, and structural connectivity of different STS regions (Habas et al. 2011; Lahnakoski et al. 2012; Shih et al. 2011; Beer et al. 2013; Blank et al. 2011; Noesselt et al. 2012; Deen et al. 2015), these studies were not particularly comprehensive, i.e., not all STS sections were evaluated, or they were narrowly focused on a specific cognitive function.

The most intensive studies of STS connections have been performed in monkeys using anatomical tracer techniques (Luppino et al. 2001; Yeterian and Pandya 1991; Seltzer and Pandya 1994, 1989; Rockland and Pandya 1981) or microstimulation (Petkov et al. 2015). However, differences may exist between human and macaque STS (Beauchamp 2005, 2012), which could potentially influence STS connectivity or coactivation maps (but see Frey et al. 2008). Thus, more examination of STS connections and coactivity is needed in humans.

Despite these shortcomings, previous studies in humans (Habas et al. 2011; Lahnakoski et al. 2012; Shih et al. 2011; Beer et al. 2013; Deen et al. 2015) and monkeys (Luppino et al. 2001; Yeterian and Pandya 1991) agree that different STS sections have distinct connectivity patterns. Dual-stream models of audition and language (Hickok and Poeppel 2007; Rauschecker and Scott 2009; Rauschecker and Tian 2000; Bornkessel-Schlesewsky et al. 2015) suggest that different STS sections might segregate based on connectivity with dorsal versus ventral pathways. Indeed other studies (Hein and Knight 2008; Liebenthal et al. 2014; Deen et al. 2015) suggest that the more posterior STS segment may have broad overlap of processes (e.g., biological motion, faces, semantic memory, etc.), whereas the more anterior segment may be more specialized to language-related processes. It is possible that the auditory and language dual-streams may be consistent across various cognitive processes that also recruit the STS. Based on these models, we hypothesized that across a broad sampling of experiments, not restricted to specific behaviors, posterior STS (pSTS) would coactivate primarily with dorsal-stream regions, whereas anterior STS (aSTS) would coactivate primarily with ventral-stream regions.

In order to identify generalizable, consistent functional coactivation patterns associated with specific sections of the STS, we tested this hypothesis using a relatively new technique called meta-analytic connectivity modeling (MACM). MACM identifies experiments that report activation foci in specific brain regions of interest (ROIs) regardless of task or behavior and uses the Activation Likelihood Estimation (ALE; Turkeltaub et al. 2002; Turkeltaub et al. 2012) coordinate-based meta-analysis method to determine the consistent whole-brain functional coactivations associated with those ROIs (Robinson et al. 2010; Zald et al. 2014; Laird et al. 2013). MACM has been used to examine functional coactivation in a number of brain areas (Cauda et al. 2011; Robinson et al. 2010; Zald et al. 2014; Robinson et al. 2012; Jakobs et al. 2012). MACM coactivation results can be compared to other measures of structural and functional connectivity, but important differences should be noted. MACM provides complementary information to resting functional connectivity and structural white matter connectivity because it captures networks of brain regions that consistently process information in conjunction with each other across various active task conditions not restricted to specific neural processes. Thus, to provide the most comprehensive examination of human STS functional coactivation across the neuroimaging literature to date, we used MACM to assess and quantitatively compare coactivation maps of bilateral anterior, middle, and posterior anatomical STS subregions across diverse experiments and behaviors.

Materials and Methods

Overview of the MACM approach

See the BrainMap website (http://brainmap.org) and previous studies (e.g., Robinson et al. 2010; Zald et al. 2014) for methodological details of MACM, which are summarized in the context of the current study below. Briefly, in the MACM method, a group of experiments that report activity within a pre-selected ROI are identified through a database search (e.g., BrainMap). Then, the ALE meta-analysis method is used on those experiments to identify areas throughout the brain that consistently coactivate with the pre-selected ROI. Thus,

MACM can be viewed as a specialized usage of the ALE method. Typical meta-analyses use ALE to identify areas of concordant activity in experiments selected to isolate a specific cognitive function or task. In contrast, MACM instead uses ALE to identify a consistent coactivation map associated with a specific brain ROI across experiments irrespective of task or behavior. In this paper, we use the term MACM to refer to the entire process of meta-analytic connectivity modeling, and use the term ALE to refer specifically to the meta-analytic algorithm used to generate the coactivation maps.

In this study, the MACM approach was applied to regions of the left and right STS. Six anatomical ROIs covering the anterior, middle, and posterior portions of bilateral STS were manually created in MNI space. Next, the BrainMap functional database (http://brainmap.org) was searched for experiments that reported activation foci located within each STS ROI. The results of these experiments, including all foci reported throughout the brain were exported. Lastly, to identify consistent coactivation patterns across experiments, ALE analyses (Turkeltaub et al. 2002; Turkeltaub et al. 2012), both single-study ("coactivation") and subtraction ALEs, were performed on the exported experiments that activated each of the six STS ROIs. The coactivation analyses identified the overall coactivation pattern for each STS subregion. The main results are reported from the subtraction analyses, which quantitatively compared STS subregion coactivation maps to identify brain regions that coactivated more for each STS subregion as compared to the other STS subregions in the same hemisphere.

Bilateral anatomical STS ROIs

Six STS ROIs were created using a combination of the lpba40 max probabilistic atlas (Shattuck et al. 2008), the AAL atlas (Tzourio-Mazoyer et al. 2002) in MRIcron (http://www.mccauslandcenter.sc.edu/mricro/mricron/), and the Colin27 template brain (Figure 1). The ROIs were drawn along the STS following the trajectory and location provided by the lpba40 max probabilistic atlas, which was overlaid on the AAL atlas and co-registered to the Colin27 brain (using SPM8, http://www.fil.ion.ucl.ac.uk/spm/software/spm8/) for additional guidance. The location of Heschl's gyrus was approximated using the AAL atlas and the Colin27 brain anatomy. The STS ROIs were manually created, and converted to nifti (.nii) image files in MRIcron.

The STS subregions were determined anatomically. Since the previous literature is inconsistent in the precise delineation of anterior versus posterior STS, and because the auditory and language dual-stream models predict that the ventral and dorsal streams emanate from primary auditory cortex (Hickok and Poeppel 2007; Rauschecker and Scott 2009; Rauschecker and Tian 2000), we divided the STS into anterior, middle and posterior subregions based on the approximate location of Heschl's gyrus. Specifically, the left and right STS were divided into six STS ROIs: left posterior STS (LpSTS), left middle STS (LmSTS), left anterior STS (LaSTS), right posterior STS (RpSTS), right middle STS (RmSTS), and right anterior STS (RaSTS). The LpSTS and RpSTS ROIs were drawn just posterior to Heschl's gyrus with approximate Y ranges of −55 to −31 (LpSTS) and −56 to −31 (RpSTS). The LmSTS and RmSTS ROIs were drawn lateral to Heschl's gyrus with approximate Y ranges of −31 to −7. The LaSTS and RaSTS ROIs were drawn anterior to

Heschl's gyrus with approximate Y ranges of −7 to 17. Following the STS trajectory and location in the lpba40 max probabilistic atlas, the depth/medial extent of the STS ROIs were drawn to the edge of the defined temporal lobe depicted in the AAL atlas with the approximate X-coordinate of −46 (left ROIs) and 45 (right ROIs). In the lpba40 max probabilistic atlas, this edge generally coincided with a medial inflection point in the STS, and the medial edge of the defined atlas for the most posterior STS regions. The lateral edge of the ROIs in some cases extended beyond the lpba40 max probabilistic atlas to regions still within the AAL atlas. The left-hemisphere ROIs were drawn to approximate X-coordinates of −69 to −46 (LpSTS and LmSTS) and −64 to −46 (LaSTS). The right-hemisphere ROIs were drawn to approximate X-coordinates of 45 to 67 (RpSTS and RmSTS) and 45 to 66 (RaSTS).

The LaSTS and RaSTS had volumes of 2784 mm^3 and 3488 mm^3, respectively. The LmSTS and RmSTS had volumes of 4400 mm^3 and 4579 mm^3, respectively. The LpSTS and RpSTS had volumes of 4329 mm^3 and 4588 mm^3, respectively. The ROIs had a voxel size of 1 mm^3. The right STS ROI volumes were slightly larger than the left STS ROI counterparts. Importantly, inter-hemispheric volumetric differences likely do not impact the main results, as the main results are the comparisons between STS subregion coactivation maps within the same hemisphere. Others have reported a depth asymmetry of the STS, where the right STS has been shown to have a deeper sulcus in the middle to posterior regions (Ochiai et al. 2004; Bonte et al. 2013; Leroy et al. 2015), regardless of handedness (Leroy et al. 2015), and overall more variability across individuals as compared to the left STS (Bonte et al. 2013). With respect to handedness, neither the lpba40 max probabilistic atlas (Shattuck et al. 2008) nor the AAL atlas (derived from a single subject; Tzourio-Mazoyer et al. 2002) reports handedness. However, the lpba40 max probabilistic atlas has an equal number of men and women, and represents various ethnicities; thus, overall the atlas has a good representative subject population.

The BrainMap functional database search

The BrainMap functional database was searched on 10/22/2013 using Sleuth, version 2.2 (Fox et al. 2005; Fox and Lancaster 2002; Laird et al. 2005b). At that time, the entire functional database contained 11,233 experiments, 2,355 papers, 45,448 subjects, and 90,159 locations. Each STS ROI was used as a search criterion, where only the experiments that reported foci within the searched STS ROI were identified. Search criteria included: STS ROI; experiments reported "activations only"; experiments were "normal mapping"; subjects were "normals"; and experiments used functional magnetic resonance imaging (fMRI) or positron emission tomography (PET) imaging modalities. In the BrainMap database, "normal mapping" experiments are classified as contrasts assessed in healthy controls only and "normal" subjects refers to controls (see thebrainmap.org website for taxonomy specifics). To ensure a broad sampling of the functional neuroimaging literature reporting activation in the STS across diverse experiments, behaviors, and tasks, no other Sleuth search restrictions were included, e.g., "paradigm class," "behavioral domain," "gender", "handedness", etc.

The search result for each STS ROI was exported to six text files of activation foci (LaSTS, LmSTS, LpSTS, RaSTS, RmSTS, RpSTS). Exported lists of foci in MNI space were grouped by experiment (Turkeltaub et al. 2012). Notably, although the experiments were identified because they reported foci within the STS ROI, all foci reported in the experiments throughout the brain were exported.

Other experimental details were exported including the behavioral categories of the experiments, and citations. Each experiment in the BrainMap database is classified into relevant behavioral categories. Experiments can be labeled with multiple behavioral classifications in BrainMap (see (http://brainmap.org) and (Laird et al. 2009) for further details). For each STS ROI, the number of experiments classified per BrainMap behavioral category is reported. Behavioral categories with zero experiments in BrainMap were not reported. As in Lancaster et al. (2012), we calculated an "other" behavioral classification to account for experiments classified in the domain but not categorized into a subcategory (i.e., we subtracted the experiment totals for each subcategory from the main category total to get the number of experiments in the "other" category). The ROI proportion of experiments classified per behavioral category compared to the BrainMap database proportion is also calculated, where the number of experiments in a behavioral category for an STS ROI out of the total number of experiments identified for that STS ROI is divided by the number of experiments in the same behavioral category in the BrainMap database out of the total number of experiments in the BrainMap database. Further, Pearson's chi squared tests with Yates' continuity correction were performed in R software (version 3.1.2), where we compared the number of experiments in a behavioral category and not in the behavioral category in an ROI vs. the number of experiments in a behavioral category and not in the behavioral category outside the ROI (i.e., rest of database). Lastly, in the supplemental material we further evaluated what behavioral categories may be statistically over-represented in each ROI, using the Mango Behavioral Analysis Plugin (Lancaster et al. 2012). This behavioral analysis was conducted on the STS ROIs accessing the BrainMap database at a later date (12–4–2015); thus it does not represent the exact group of experiments used in this MACM study. Nevertheless, it still can be used to determine whether activity associated with specific behavioral categories in the BrainMap database is more likely to occur within our ROIs than elsewhere in the brain.

ALE analyses: Coactivations

The ALE method is a meta-analytic technique that models the uncertainty in localization of activation foci as 3-dimensional Gaussian probability distributions and combines these distributions across neuroimaging experiments to determine brain regions of consistent activation; see previous published work for details (Turkeltaub et al. 2002; Turkeltaub et al. 2012; Eickhoff et al. 2009; Eickhoff et al. 2012). To assess whole-brain coactivations for each STS subregion, we performed six single-study "coactivation" ALE analyses on the lists of foci exported from BrainMap as described above (LaSTS, LmSTS, LpSTS, RaSTS, RmSTS, RpSTS). These analyses produced maps of the areas throughout the brain that consistently activated during experiments that also activated subregions of the STS. All ALE analyses were conducted using GingerALE version 2.3.1 (http://brainmap.org) and using the "Turkeltaub Non-Additive" ALE method (Turkeltaub et al. 2012). All coactivation ALE

analyses are reported with a false discovery rate (FDR; Laird et al. 2005a) of 0.001, and cluster threshold of 100 mm^3.

Main ALE analyses: Subtractions

For our main results, we quantitatively compared the coactivation maps of different STS subregions because some experiments reported foci in more than one STS subregion and the STS subregions displayed some overlap in coactivation. We performed a series of ALE subtraction analyses (Eickhoff et al. 2011) to identify the brain areas that were more consistently coactivated with one STS subregion as compared to the other two STS subregions in the same hemisphere. These contrast analyses allowed for the assessment of coactivation pattern specificity for one STS subregion compared to the rest of the STS in the same hemisphere. The following six ALE subtractions were conducted: 1) LaSTS > (LmSTS & LpSTS); 2) LmSTS > (LaSTS & LpSTS); 3) LpSTS > (LaSTS & LmSTS); 4) RaSTS > (RmSTS & RpSTS); 5) RmSTS > (RaSTS & RpSTS); and 6) RpSTS > (RaSTS & RmSTS). Since the number of experiments identified for each STS subregion varied, it is important to note that the subtraction ALE analysis uses a permutation significance test that takes into account differences in experiment number on each side of the subtraction (Eickhoff et al. 2011; http://brainmap.org). All subtraction ALE analyses were performed with 10,000 permutations, and are reported with an FDR (Laird et al. 2005a) of 0.05 and cluster threshold of 100 mm^3.

Figures were created using MRIcron. Figures 2–5 present results shown on rendered and representative axial slices of the Colin27 template brain. All anatomical locations were determined using a combination of the AAL atlas via MRIcron, and the Colin27 brain anatomy. Coordinates are reported in MNI space.

Results

STS search results from the BrainMap functional database

The BrainMap search results for the six STS ROI searches are reported in Table 1. For the left STS, 434 unique experiments comprising 6071 subjects and 6415 foci were identified. For the right STS, 435 unique experiments comprising 6021 subjects and 6659 foci were identified. The number of unique experiments was defined as the number of experiments only counted once even if activations were identified in more than one STS ROI in that same hemisphere. Notably, some experiments were identified for more than one STS ROI, because they reported activation foci in more than one STS ROI. These experiments were not excluded from the analyses, because it would bias the results in favor of experiments that only reported activity within a single STS subregion, which would not be representative of the pattern of activity or the entire literature. To address this issue, the subtraction ALE analyses are reported as the main results of this study, which were conducted to isolate coactivation patterns specific to an STS subregion. Importantly, the majority of experiments in each STS ROI did not report activations in other ROIs in the same hemisphere, suggesting that there should be good power to detect coactivation differences across the ROIs in the subtraction analyses.

The search criteria for experiments that reported activations in each of the STS ROIs were broad and search results were not restricted to a specific behavior. Thus, experiments identified for each STS subregion spanned a variety of behavioral categories. As expected, some behaviors had a larger proportion of experiments in the ROIs than in the BrainMap database as a whole (Table 2 and Table 3), reflecting some functional specialization within the ROIs, particularly for language and audition, but other categories as well. This relative functional specialization was also assessed with additional behavioral analyses on the STS ROIs accessing the BrainMap database at a later date (12–4–2015) using the Mango Behavioral Analysis plugin (Lancaster et al. 2012; Supplemental Table 1). Here, LmSTS, LpSTS and RpSTS subregions were associated with language behavioral categories and LpSTS and RmSTS were associated with the auditory behavioral category. However, these assessments are reflective of relative over-representation of these functions compared to the rest of the brain and the BrainMap database as a whole. Importantly, in absolute terms for each STS ROI, a substantial number of experiments included in the analyses involved other functions. Overall, numerous behavioral categories per STS ROI were represented. This suggests that the results observed for each STS subregion may generalize to various kinds of behavioral experiments.

Coactivation patterns of left STS subregions

ALE analyses examining coactivation patterns across the brain associated with the three left STS subregions revealed overlapping coactivation to varying degrees in the left frontal areas including the inferior frontal gyrus (IFG), precentral gyrus, and supplementary motor area (SMA), as well as regions in bilateral insula (Figure 2). This overlap may partly be related to experiments reporting activations in two (50 experiments) or three (5 experiments) left STS subregions. The LpSTS showed more bilateral and extensive coactivation of frontal areas, particularly the auditory and language dorsal-stream regions. Each left STS subregion displayed coactivation with the right superior temporal gyrus (STG) extending through the STS and into the middle temporal gyrus (MTG), generally including some areas relatively homotopic to that left STS subregion. Both the LpSTS and LaSTS had coactivation peaks in visual ventral-stream areas in left fusiform gyrus (FFG). Only the LpSTS had coactivation peaks in bilateral thalamus, and in auditory and language dorsal-stream regions in bilateral parietal areas including inferior parietal lobule (IPL). The LaSTS and LmSTS coactivated with the left superior parietal lobule (SPL) but to a much smaller degree. Coactivation peaks only found for the LaSTS were observed in the left midbrain, left amygdala, and right calcarine cortex (V1). In summary, while there were some regions of overlap, distinct coactivation patterns were revealed for different subregions of the left STS.

Left STS subtractions: Coactivation patterns specific to each left STS subregion

To determine brain regions that were more consistently coactivated with one left STS subregion as compared to the other two, we conducted three ALE subtraction analyses (Figure 3, Table 4): 1) LpSTS > (LaSTS & LmSTS), 2) LaSTS > (LmSTS & LpSTS), and 3) LmSTS > (LaSTS & LpSTS). Critically, these contrasts allowed for the isolation of coactivation patterns specific to that subregion in the context of the rest of the STS in the same hemisphere. Across the whole brain, several auditory and language dorsal-stream regions coactivated more with the LpSTS as compared to the LaSTS and LmSTS.

Coactivation peaks included bilateral IPL, SMA, left precentral gyrus, right middle frontal gyrus (MFG), and right posterior STG/MTG. Coactivation peaks in the right IFG pars opercularis and orbitalis were also identified (note that while pars opercularis is considered part of the dorsal stream, pars orbitalis is generally considered part of the ventral stream). Compared to LmSTS and LpSTS, the LaSTS coactivated more with the right STG/MTG pole, left hippocampus extending in the amygdala, left midbrain, left cerebellum, and right cuneus. LaSTS compared to RaSTS had more coactivation with only one region in the left posterior MTG (Supplemental Figure 3). The LmSTS as compared to the LaSTS and LpSTS coactivated more with a small number of regions including peaks in the right middle STS and left calcarine cortex (V1). Notably, none of the left STS subtractions revealed coactivation peaks with the left IFG, perhaps due to extensive overlap of left STS subregion coactivation maps at that location. However, more coactivation was identified in the left IFG for LpSTS as compared to RpSTS (Supplemental Figure 1) and for LmSTS as compared to RmSTS (Supplemental Figure 2).

Coactivation patterns of right STS subregions

The right STS coactivation patterns were determined using the same method as the left STS. In general, the left and right homotopic STS subregions had similar coactivation patterns, e.g., within the left frontal and temporal areas (Figure 4). There was also similar overlap across right STS subregion coactivation maps, which may in part be related to some experiments that reported activations in two (54 experiments) or three (5 experiments) of the right STS subregions. Qualitative differences between the left and right STS coactivation patterns were also identified. For example, generally the RpSTS and RmSTS had qualitatively more extensive coactivation in the right frontal areas compared to other STS subregions. Also, the RpSTS had coactivation peaks in visual dorsal-stream regions in the right MTG, visual ventral-stream regions in bilateral FFG, as well as bilateral hippocampi extending into the amygdalae. The RmSTS also coactivated with the left FFG. To summarize, the right and left homotopic STS subregions had generally similar coactivation patterns, with some qualitative differences (see Supplemental Figures 1–3 for quantitative ALE comparisons between left and right STS subregions).

Right STS subtractions: Coactivation patterns specific to each right STS subregion

Similar to the left STS, three ALE subtraction analyses were conducted on the right STS (Figure 5, Table 5): 1) RpSTS > (RaSTS & RmSTS), 2) RaSTS > (RmSTS & RpSTS), 3) RmSTS > (RaSTS & RpSTS). Similar to the LpSTS, the RpSTS had more coactivation peaks as compared to the RaSTS and RmSTS in several auditory and language dorsal-stream regions, such as bilateral precentral gyrus, SMA, and the homotopic posterior STG/MTG, as well as in the right IFG pars opercularis and orbitalis (homotopic to a ventral-stream region). The RpSTS also had more coactivation with the right MTG in the vicinity of human MT+, the visual motion complex (Huk et al. 2002; Malikovic et al. 2007), and the right amygdala. While the LpSTS subtraction ALE identified more coactivation with bilateral IPL, no IPL coactivation peaks were found for the RpSTS subtraction ALE. However, RpSTS compared to LpSTS had more coactivation in right supramarginal gyrus (Supplemental Figure 1). The RaSTS as compared to the RmSTS and RpSTS had more coactivation only in two auditory and language ventral-stream regions, one large coactivation cluster with ALE peaks in the

left anterior MTG and in the left IFG pars orbitalis. No other coactivation peaks were identified. Notably, none of the other left or right STS subtractions across ROIs in the same hemisphere identified coactivation peaks with the left IFG. Additionally, the RaSTS as compared to the LaSTS had more coactivation in bilateral posterior temporal regions (Supplemental Figure 3). The RmSTS had more coactivation as compared to the RaSTS and RpSTS in a cluster with ALE peaks in the left middle MTG and left Heschl's gyrus, and a cluster with ALE peaks in the left precentral gyrus and in the postcentral gyrus. The RmSTS as compared to the LmSTS had more coactivation in multiple areas including bilateral subcortical areas, bilateral IPL, and the left calcarine cortex (Supplemental Figure 2).

Discussion

Using the MACM approach, we identified distinct coactivation patterns for anterior, middle, and posterior anatomical STS subregions across experiments examining diverse behaviors. Quantitative ALE contrasts were conducted to determine the areas with more coactivation associated with each STS subregion, since substantial coactivation overlap, mostly in the frontal and temporal lobe, was identified among STS subregions. Our main findings revealed that across various experiments and behaviors pSTS coactivated more strongly than other STS subregions in the same hemisphere with auditory and language dorsal-stream regions. In contrast, aSTS coactivated more with some auditory and language ventral-stream regions, albeit less robustly. The homotopic left and right STS subregions displayed relatively similar coactivation patterns with some differences noted. Overall, by providing consistent and generalizable coactivation maps for STS subregions in humans across various experiments and behaviors, these findings have broad applicability for future studies and underscore the utility of nonhuman primate models for the study of brain organization in humans.

Generalized STS coactivation with auditory language dual streams

In general, across various behaviors the pSTS robustly displayed more coactivation with auditory and language dorsal-stream regions, whereas the aSTS displayed more coactivation with some ventral-stream regions. These findings support the hypothesis of segregated dual pathways for auditory and language processing in humans (Hickok and Poeppel 2007; Rauschecker and Scott 2009), which is based on analogous findings in nonhuman primates (Romanski et al. 1999; Rauschecker and Tian 2000; Tian et al. 2001). Rauschecker and Scott (2009) proposed a dualstream model where the ventral stream performs auditory object recognition (e.g., the identification of speech sounds; Leaver and Rauschecker 2010; DeWitt and Rauschecker 2012) and includes the "rostral belt" auditory cortex (Kaas and Hackett 2000; Rauschecker and Tian 2000), anterior superior temporal cortex (STC) and ventral IFG. The dorsal stream processes sensorimotor and spatial signals, implementing predictive coding mechanisms (forward models), and includes the "caudal belt" auditory cortex (Kaas and Hackett 2000; Rauschecker and Tian 2000), posterior STC, IPL, premotor areas, and the dorsal IFG. The Hickok and Poeppel (2007) language dual-stream model is also consistent with our findings. This model proposed that the dorsal and ventral streams interact with bilateral middle to posterior STS regions, which are hypothesized to process phonological information (Hickok and Poeppel 2007). These processing streams may accommodate other functions and processes as well (Rauschecker and Scott 2009; see also Warren et al. 2005),

which could help to explain the overlap of numerous STS functions in more posterior regions (Hein and Knight 2008; Liebenthal et al. 2014; Deen et al. 2015), as well as the coactivation patterns presented here representing various behaviors. The suggestion that STS coactivations may be related to dorsal/ventral streams is hardly surprising when considering that dual-stream models are proposed for various neural processes including audition, language, and vision (see review Cloutman 2013), all of which are associated with the STS (Hein and Knight 2008). In our assessment of STS coactivation patterns, we aimed to identify generalizable coactivation patterns and did not restrict our analyses to specific experiment types targeting distinct neural processes. In our findings, while aSTS coactivation with ventral-stream regions is less strong and could benefit from future examinations, the robust finding that pSTS consistently coactivated more with dorsal-stream regions across various behaviors further suggests a more general role for this processing stream.

The auditory/language dorsal-stream coactivation with pSTS and ventral-stream coactivation with aSTS reported in our study is well supported in the literature and complement previous connectivity findings in humans and nonhuman primates. Buchsbaum et al. (2005) reported that an auditory memory region in the planum temporale had more task-related functional connectivity with dorsal-stream regions, whereas a more anterior auditory memory region in mid-STG/STS had more functional connectivity with ventral-stream regions. Frey et al. (2008) reported structural evidence suggesting that the middle/inferior longitudinal fasciculus connected posterior STC and parietal regions, and the superior longitudinal fasciculus connected parietal regions and the posterior part of Broca's area (BA44). In addition, direct connections were found between posterior STC and BA44 in both humans and monkeys (Frey et al. 2008; Frey et al. 2014). By contrast, the extreme capsule connected anterior to mid-STG/STS and the anterior part of Broca's area (BA45) (Frey et al. 2008). Recently, microstimulation studies in monkeys (Petkov et al. 2015) have demonstrated that the aSTS region is most tightly connected with a region in ventrolateral prefrontal cortex. A human atlas based on diffusion MRI tractography findings (Catani and Thiebaut de Schotten 2012) suggests that pSTS may overlap with the posterior segment of the arcuate fasciculus, which likely connects dorsal-stream regions. In a recent ALE meta-analysis of conflicting AV speech signals, we found significant activation likelihoods in dorsal-stream regions including SMA and left IPL along with bilateral pSTS (Erickson et al. 2014).

Previous studies have examined connectivity of different STS subregions (Habas et al. 2011; Lahnakoski et al. 2012; Shih et al. 2011; Beer et al. 2013; Blank et al. 2011; Noesselt et al. 2012; Deen et al. 2015). Some connectivity with dorsal and ventral streams has been reported, including pSTS resting functional connectivity with dorsal-stream regions, such as SMA, precentral gyrus, and parietal cortex (Habas et al. 2011), pSTS steady-state functional connectivity with frontal and parietal regions in control children and adolescents (Shih et al. 2011), and white-matter tracts connecting pSTS to parietal and frontal areas (Beer et al. 2013). A study of task-based functional connectivity associated with social processes demonstrated connectivity of pSTS with premotor cortex and MT+/V5, as well as other areas outside of the dorsal/ventral streams (see below; Lahnakoski et al. 2012). In parallel with our results, Deen et al. (2015) found similar resting functional connectivity patterns for aSTS and pSTS using a pSTS seed region derived from a contrast of biological motion and

an aSTS seed region derived from a contrast of language. Lastly, evidence from monkeys suggests that rostral vs. caudal STS has different connections with frontal cortex, i.e., F6/F7 and F7/F2, respectively (Luppino et al. 2001).

Generalized STS coactivations with brain regions associated with other STS functions

In this study, we found that other regions outside of the canonical auditory and language dorsal/ventral areas coactivated with the STS. It is likely that STS connectivity is more complex than a simple anterior to posterior division into dorsal and ventral streams, since the STS is involved in other neural processes (see STS review by Hein and Knight (2008)). Hein and Knight (2008) suggested that differential STS network coactivations might be critical in understanding how the STS is involved in various neural processes. Some of our findings support coactivations associated with other STS neural processes, some related to audition and language, others less so. For example, the auditory/language dual-stream models do not explicitly discuss AV integration, but since there is clear evidence that the STS is involved in AV processes (Beauchamp et al. 2004; Beauchamp et al. 2010), some coactivation between STS and early auditory and visual areas can be expected (Powers et al. 2012; Noesselt et al. 2007; Nath and Beauchamp 2011; Beer et al. 2013). Indeed, our study did identify STS coactivation with early visual and auditory areas, e.g., the LmSTS showed more coactivation with the left calcarine cortex (VI), and the RmSTS showed more coactivation with left Heschl's gyrus.

Less directly related to audition/language, the STS is involved in processing biological motion (Giese and Poggio 2003) and faces (Haxby et al. 2000). Giese and Poggio (2003) proposed that the STS was part of the "form" and "motion" biological motion pathways, receiving input from V4 and MT+, respectively. The cerebellum has also been reported in biological motion processing (Grossman et al. 2000), and others have shown that the left cerebellum has connectivity with the right STS (Sokolov et al. 2014; Sokolov et al. 2012). Haxby et al. (2000) proposed that the STS, FFG, and inferior occipital gyri were part of the "core" face network, where the pSTS processes "changeable aspects of faces," e.g., "dynamic facial expressions" (Said et al. 2010). Several studies have reported structural and functional connectivity between the STS and FFG (Zhang et al. 2009; Turk-Browne et al. 2010; Blank et al. 2011; Lahnakoski et al. 2012). Our findings generally support these previous connectivity findings, identifying coactivation between the RpSTS and right MT+, between several STS subregions and the cerebellum, and between some STS subregions and FFG.

The STS and amygdala have been implicated in social perception processes (Allison et al. 2000). Structural connections between the STS and amygdala have been identified (Grezes et al. 2014; Iidaka et al. 2012). Lahnakoski et al. (2012) investigated the functional network related to social processing and found that different STS regions were connected to various areas, e.g., the aSTS showed functional connectivity with the amygdala, and the RpSTS showed functional connectivity with the right insula, right premotor cortex, right FFG, bilateral MT+/V5, and other STS subregions. In the present study, the LaSTS and RpSTS both had more coactivation with the amygdala, as compared to the other STS subregions in the same hemisphere.

Limitations

While this study provides strong evidence for differential functional coactivation of STS subregions, there are some other points to consider. First, we focused exclusively on the STS here since research in various cognitive and perceptual domains has specifically identified it as an important processing region (Hein and Knight 2008). However, macrostructural anatomical features (e.g., gyri, sulci) do not generally coincide with functionally specialized processing units. Also, the STS ROIs were subdivided anatomically using somewhat arbitrary boundaries. While there is some evidence for various STS functional subregions (Stevenson and James 2009; Beauchamp et al. 2004; Noesselt et al. 2012; Shih et al. 2011; Liebenthal et al. 2014; Deen et al. 2015), these studies are not conclusive. To provide a more complete examination of functional specialization and network connectivity in the region, future studies are needed to comprehensively test the possibility of functional subregions along the entire STS including neighboring areas of lateral temporal cortex, using data-driven parcellation techniques, such as coactivation-based parcellation, or other methods (Turk-Browne et al. 2010). Additionally, the STS is a complex structure that has varied sulcal patterns across individuals (Ochiai et al. 2004) and may be obscured during normalization. This issue is common to STS studies and is perhaps strained when performing a meta-analysis. We addressed this issue by utilizing a probabilistic atlas (lpba40; Shattuck et al. 2008) to best estimate the trajectory and location of the STS. Lastly, the results more convincingly support pSTS coactivation with dorsal-stream regions than aSTS with ventral-stream regions. This may be related to the disproportionate number of experiments identified for pSTS (left: 255, right: 215) compared to aSTS (left: 78, right: 92), perhaps due to differences in ROI size.

Conclusions

Using the MACM approach, differential task-based functional coactivation patterns were revealed for bilateral anatomical STS subregions across experiments examining various behaviors. To the best of our knowledge, this is the first comprehensive, meta-analytic assessment of human STS functional coactivations. In general, across experiments and behaviors, the pSTS strongly coactivated with dorsal-stream regions, whereas the aSTS coactivated with some ventral-stream regions, as predicted by auditory/language dual-stream models (Hickok and Poeppel 2007; Rauschecker and Scott 2009; Rauschecker and Tian 2000). Other STS coactivations outside of the dorsal/ventral streams were identified. These STS MACM findings have a broad relevance for future studies including those testing the hypothesized connectivity for various functions of the STS, as well as the potential to influence future unified STS processing models incorporating its multiple functions.

Supplementary Material

Refer to Web version on PubMed Central for supplementary material.

Compliance with Ethical Standards:

Acknowledgments

This material is based upon work supported by the National Science Foundation (NSF) Graduate Research Fellowship Program under Grant Nos. DGE-0903443 and DGE-1444316 (to LCE) as well as the Achievement

Rewards for College Scientists Metropolitan Washington Chapter Scholar 2015–2016 (to LCE). This work was supported by grants from the National Institutes of Health (KL2TR000102 to PET; R01-DC03489, R01-NS052494 and R56-NS052494 to JPR), Doris Duke Charitable Foundation (2012062 to PET), the Vernon Family Trust (PET), and a PIRE grant from the NSF (OISE-0730255 to JPR). We would like to thank Rachel Acree and Elizabeth Heeg for their help working with the data.

References

Allison T, Puce A, McCarthy G. Social perception from visual cues: role of the STS region Trends Cogn Sci. 2000; 4(7):267–278. DOI: 10.1016/S1364-6613(00)01501-1 [PubMed: 10859571]

Beauchamp MS. See me, hear me, touch me: multisensory integration in lateral occipital-temporal cortex Curr Opin Neurobiol. 2005; 15(2):145–153. DOI: 10.1016/j.conb.2005.03.011 [PubMed: 15831395]

Beauchamp MS. Adams RB. Biological Motion and Multisensory Integration: The Role of the Superior Temporal Sulcus The Science of Social Vision: The Science of Social Vision. 2011; 7:409–420.

Beauchamp MS, (2012) Multisensory integration in the human superior temporal sulcus In: Stein BE. (ed) The New Handbook of Multisensory Processing . pp 179–191

Beauchamp MS. The social mysteries of the superior temporal sulcus Trends Cogn Sci. 2015; 19(9): 489–490. DOI: 10.1016/j.tics.2015.07.002 [PubMed: 26208834]

Beauchamp MS, Argall BD, Bodurka J, Duyn JH, Martin A. Unraveling multisensory integration: patchy organization within human STS multisensory cortex Nat Neurosci. 2004; 7(11):1190–1192. DOI: 10.1038/Nn1333 [PubMed: 15475952]

Beauchamp MS, Nath AR, Pasalar S. fMRI-Guided Transcranial Magnetic Stimulation Reveals That the Superior Temporal Sulcus Is a Cortical Locus of the McGurk Effect J Neurosci. 2010; 30(7): 2414–2417. DOI: 10.1523/Jneurosci.4865-09.2010 [PubMed: 20164324]

Beer AL, Plank T, Greenlee MW. Diffusion tensor imaging shows white matter tracts between human auditory and visual cortex Exp Brain Res. 2011; 213(2–3):299–308. DOI: 10.1007/S00221-011-2715-Y [PubMed: 21573953]

Beer AL, Plank T, Meyer G, Greenlee MW. Combined diffusion-weighted and functional magnetic resonance imaging reveals a temporal-occipital network involved in auditory-visual object processing Front Integr Neurosci. 2013; 7:5.doi: 10.3389/fnint.2013.00005 [PubMed: 23407860]

Bernstein LE, Liebenthal E. Neural pathways for visual speech perception Front Neurosci. 2014; 8:386.doi: 10.3389/fnins.2014.00386 [PubMed: 25520611]

Bishop CW, Miller LM. A Multisensory Cortical Network for Understanding Speech in Noise J Cogn Neurosci. 2009; 21(9):1790–1804. DOI: 10.1162/Jocn.2009.21118 [PubMed: 18823249]

Blank H, Anwander A, von Kriegstein K. Direct Structural Connections between Voice- and Face-Recognition Areas J Neurosci. 2011; 31(36):12906–12915. DOI: 10.1523/Jneurosci.2091-11.2011 [PubMed: 21900569]

Bonte M, Frost MA, Rutten S, Ley A, Formisano E, Goebel R. Development from childhood to adulthood increases morphological and functional inter-individual variability in the right superior temporal cortex Neuroimage. 2013; 83:739–750. DOI: 10.1016/j.neuroimage.2013.07.017 [PubMed: 23867553]

Bornkessel-Schlesewsky I, Schlesewsky M, Small SL, Rauschecker JP. Neurobiological roots of language in primate audition: common computational properties Trends Cogn Sci. 2015; doi: 10.1016/j.tics.2014.12.008

Buchsbaum BR, Olsen RK, Koch P, Berman KF. Human dorsal and ventral auditory streams subserve rehearsal-based and echoic processes during verbal working memory Neuron. 2005; 48(4):687–697. DOI: 10.1016/J.Neuron.2005.09.029 [PubMed: 16301183]

Catani M, Thiebaut de Schotten M. (2012) Atlas of Human Brain Connections . Oxford University Press ,

Cauda F, Cavanna AE, D'Agata F, Sacco K, Duca S, Geminiani GC. Functional connectivity and coactivation of the nucleus accumbens: a combined functional connectivity and structure-based meta-analysis J Cogn Neurosci. 2011; 23(10):2864–2877. DOI: 10.1162/jocn.2011.21624 [PubMed: 21265603]

Cloutman LL. Interaction between dorsal and ventral processing streams: where, when and how? Brain Lang. 2013; 127(2):251–263. DOI: 10.1016/j.bandl.2012.08.003 [PubMed: 22968092]

Deen B, Koldewyn K, Kanwisher N, Saxe R. Functional Organization of Social Perception and Cognition in the Superior Temporal Sulcus Cereb Cortex. 2015; 25(11):4596–4609. DOI: 10.1093/cercor/bhv111 [PubMed: 26048954]

Deen B, Pitskel NB, Pelphrey KA. Three Systems of Insular Functional Connectivity Identified with Cluster Analysis Cereb Cortex. 2011; 21(7):1498–1506. DOI: 10.1093/Cercor/Bhq186 [PubMed: 21097516]

DeWitt I, Rauschecker JP. Phoneme and word recognition in the auditory ventral stream Proc Natl Acad Sci U S A. 2012; 109(8):E505–514. DOI: 10.1073/pnas.1113427109 [PubMed: 22308358]

Driver J, Noesselt T. Multisensory interplay reveals crossmodal influences on 'sensory-specific' brain regions, neural responses, and judgments Neuron. 2008; 57(1):11–23. DOI: 10.1016/J.Neuron.2007.12.013 [PubMed: 18184561]

Eickhoff SB, Bzdok D, Laird AR, Kurth F, Fox PT. Activation likelihood estimation meta-analysis revisited Neuroimage. 2012; 59(3):2349–2361. DOI: 10.1016/J.Neuroimage.2011.09.017 [PubMed: 21963913]

Eickhoff SB, Bzdok D, Laird AR, Roski C, Caspers S, Zilles K, Fox PT. Co-activation patterns distinguish cortical modules, their connectivity and functional differentiation Neuroimage. 2011; 57(3):938–949. DOI: 10.1016/J.Neuroimage.2011.05.021 [PubMed: 21609770]

Eickhoff SB, Laird AR, Grefkes C, Wang LE, Zilles K, Fox PT. Coordinate-Based Activation Likelihood Estimation Meta-Analysis of Neuroimaging Data: A Random-Effects Approach Based on Empirical Estimates of Spatial Uncertainty Hum Brain Mapp. 2009; 30(9):2907–2926. DOI: 10.1002/Hbm.20718 [PubMed: 19172646]

Erickson LC, Heeg E, Rauschecker JP, Turkeltaub PE. An ALE meta-analysis on the audiovisual integration of speech signals Hum Brain Mapp. 2014; 35(11):5587–5605. DOI: 10.1002/hbm.22572 [PubMed: 24996043]

Fox PT, Laird AR, Fox SP, Fox PM, Uecker AM, Crank M, Koenig SF, Lancaster JL. BrainMap taxonomy of experimental design: Description and evaluation Hum Brain Mapp. 2005; 25(1):185–198. DOI: 10.1002/Hbm.20141 [PubMed: 15846810]

Fox PT, Lancaster JL. Mapping context and content: the BrainMap model Nat Rev Neurosci. 2002; 3(4):319–321. DOI: 10.1038/Nrn789 [PubMed: 11967563]

Frey S, Campbell JS, Pike GB, Petrides M. Dissociating the human language pathways with high angular resolution diffusion fiber tractography J Neurosci. 2008; 28(45):11435–11444. DOI: 10.1523/JNEUROSCI.2388-08.2008 [PubMed: 18987180]

Frey S, Mackey S, Petrides M. Cortico-cortical connections of areas 44 and 45B in the macaque monkey Brain Lang. 2014; 131:36–55. DOI: 10.1016/J.Bandl.2013.05.005 [PubMed: 24182840]

Giese MA, Poggio T. Neural mechanisms for the recognition of biological movements Nat Rev Neurosci. 2003; 4(3):179–192. DOI: 10.1038/Nrn1057 [PubMed: 12612631]

Grezes J, Valabregue R, Gholipour B, Chevallier C. A direct amygdala-motor pathway for emotional displays to influence action: A diffusion tensor imaging study Hum Brain Mapp. 2014; 35(12):5974–5983. DOI: 10.1002/hbm.22598 [PubMed: 25053375]

Grossman E, Donnelly M, Price R, Pickens D, Morgan V, Neighbor G, Blake R. Brain areas involved in perception of biological motion J Cogn Neurosci. 2000; 12(5):711–720. DOI: 10.1162/089892900562417 [PubMed: 11054914]

Habas C, Guillevin R, Abanou A. Functional connectivity of the superior human temporal sulcus in the brain resting state at 3T Neuroradiology. 2011; 53(2):129–140. DOI: 10.1007/S00234-010-0775-5 [PubMed: 20924756]

Haxby JV, Hoffman EA, Gobbini MI. The distributed human neural system for face perception Trends Cogn Sci. 2000; 4(6):223–233. DOI: 10.1016/S1364-6613(00)01482-0 [PubMed: 10827445]

Hein G, Knight RT. Superior Temporal Sulcus-It's My Area: Or Is It? J Cogn Neurosci. 2008; 20(12):2125–2136. DOI: 10.1162/Jocn.2008.20148 [PubMed: 18457502]

Hickok G, Poeppel D. The cortical organization of speech processing Nat Rev Neurosci. 2007; 8(5):393–402. DOI: 10.1038/nrn2113 [PubMed: 17431404]

Huk AC, Dougherty RF, Heeger DJ. Retinotopy and functional subdivision of human areas MT and MST J Neurosci. 2002; 22(16):7195–7205. [PubMed: 12177214]

Iacoboni M. Neural mechanisms of imitation Curr Opin Neurobiol. 2005; 15(6):632–637. DOI: 10.1016/j.conb.2005.10.010 [PubMed: 16271461]

Iacoboni M, Dapretto M. The mirror neuron system and the consequences of its dysfunction Nat Rev Neurosci. 2006; 7(12):942–951. DOI: 10.1038/nrn2024 [PubMed: 17115076]

Iidaka T, Miyakoshi M, Harada T, Nakai T. White matter connectivity between superior temporal sulcus and amygdala is associated with autistic trait in healthy humans Neurosci Lett. 2012; 510(2):154–158. DOI: 10.1016/J.Neulet.2012.01.029 [PubMed: 22285821]

Jakobs O, Langner R, Caspers S, Roski C, Cieslik EC, Zilles K, Laird AR, Fox PT, Eickhoff SB. Across-study and within-subject functional connectivity of a right temporoparietal junction subregion involved in stimulus-context integration Neuroimage. 2012; 60(4):2389–2398. DOI: 10.1016/j.neuroimage.2012.02.037 [PubMed: 22387170]

Kaas JH, Hackett TA. Subdivisions of auditory cortex and processing streams in primates Proc Natl Acad Sci U S A. 2000; 97(22):11793–11799. DOI: 10.1073/pnas.97.22.11793 [PubMed: 11050211]

Lahnakoski JM, Glerean E, Salmi J, Jaaskelainen I, Sams M, Hari R, Nummenmaa L. Naturalistic fMRI mapping reveals superior temporal sulcus as the hub for the distributed brain network for social perception Front Hum Neurosci. 2012; 6doi: 10.3389/Fnhum.2012.00233

Laird AR, Eickhoff SB, Kurth F, Fox PM, Uecker AM, Turner JA, Robinson JL, Lancaster JL, Fox PT. ALE Meta-Analysis Workflows Via the Brainmap Database: Progress Towards A Probabilistic Functional Brain Atlas Front Neuroinform. 2009; 3:23.doi: 10.3389/neuro.11.023.2009 [PubMed: 19636392]

Laird AR, Eickhoff SB, Rottschy C, Bzdok D, Ray KL, Fox PT. Networks of task coactivations Neuroimage. 2013; 80:505–514. DOI: 10.1016/J.Neuroimage.2013.04.073 [PubMed: 23631994]

Laird AR, Fox PM, Price CJ, Glahn DC, Uecker AM, Lancaster JL, Turkeltaub PE, Kochunov P, Fox PT. ALE meta-analysis: Controlling the false discovery rate and performing statistical contrasts Hum Brain Mapp. 2005a; 25(1):155–164. DOI: 10.1002/Hbm.20136 [PubMed: 15846811]

Laird AR, Lancaster JL, Fox PT. BrainMap - The social evolution of a human brain mapping database Neuroinformatics. 2005b; 3(1):65–77. DOI: 10.1385/Ni:3:1:065 [PubMed: 15897617]

Lancaster JL, Laird AR, Eickhoff SB, Martinez MJ, Fox PM, Fox PT. Automated regional behavioral analysis for human brain images Front Neuroinform. 2012; 6:23.doi: 10.3389/fninf.2012.00023 [PubMed: 22973224]

Leaver AM, Rauschecker JP. Cortical representation of natural complex sounds: effects of acoustic features and auditory object category J Neurosci. 2010; 30(22):7604–7612. DOI: 10.1523/JNEUROSCI.0296-10.2010 [PubMed: 20519535]

Leroy F, Cai Q, Bogart SL, Dubois J, Coulon O, Monzalvo K, Fischer C, Glasel H, Van der Haegen L, Benezit A, Lin CP, Kennedy DN, Ihara AS, Hertz-Pannier L, Moutard ML, Poupon C, Brysbaert M, Roberts N, Hopkins WD, Mangin JF, Dehaene-Lambertz G. New human-specific brain landmark: The depth asymmetry of superior temporal sulcus Proc Natl Acad Sci U S A. 2015; 112(4):1208–1213. DOI: 10.1073/pnas.1412389112 [PubMed: 25583500]

Liebenthal E, Desai RH, Humphries C, Sabri M, Desai A. The functional organization of the left STS: a large scale meta-analysis of PET and fMRI studies of healthy adults Front Neurosci. 2014; 8:289.doi: 10.3389/fnins.2014.00289 [PubMed: 25309312]

Luppino G, Calzavara R, Rozzi S, Matelli M. Projections from the superior temporal sulcus to the agranular frontal cortex in the macaque Eur J Neurosci. 2001; 14(6):1035–1040. [PubMed: 11595042]

Malikovic A, Amunts K, Schleicher A, Mohlberg H, Eickhoff SB, Wilms M, Palomero-Gallagher N, Armstrong E, Zilles K. Cytoarchitectonic analysis of the human extrastriate cortex in the region of V5/MT+: A probabilistic, stereotaxic map of area h0c5 Cereb Cortex. 2007; 17(3):562–574. DOI: 10.1093/Cercor/Bhj181 [PubMed: 16603710]

Margulies DS, Petrides M. Distinct Parietal and Temporal Connectivity Profiles of Ventrolateral Frontal Areas Involved in Language Production J Neurosci. 2013; 33(42):16846–16852. DOI: 10.1523/Jneurosci.2259-13.2013 [PubMed: 24133284]

Nath AR, Beauchamp MS. Dynamic Changes in Superior Temporal Sulcus Connectivity during Perception of Noisy Audiovisual Speech J Neurosci. 2011; 31(5):1704–1714. DOI: 10.1523/Jneurosci.4853-10.2011 [PubMed: 21289179]

Noesselt T, Bergmann D, Heinze HJ, Munte T, Spence C. Coding of multisensory temporal patterns in human superior temporal sulcus Front Integr Neurosci. 2012; 6:64.doi: 10.3389/fnint.2012.00064 [PubMed: 22973202]

Noesselt T, Rieger JW, Schoenfeld MA, Kanowski M, Hinrichs H, Heinze HJ, Driver J. Audiovisual temporal correspondence modulates human multisensory superior temporal sulcus plus primary sensory cortices J Neurosci. 2007; 27(42):11431–11441. DOI: 10.1523/Jneurosci.2252-07.2007 [PubMed: 17942738]

Ochiai T, Grimault S, Scavarda D, Roch G, Hori T, Riviere D, Mangin JF, Regis J. Sulcal pattern and morphology of the superior temporal sulcus Neuroimage. 2004; 22(2):706–719. DOI: 10.1016/J.Neuroimage.2004.01.023 [PubMed: 15193599]

Petkov CI, Kikuchi Y, Milne AE, Mishkin M, Rauschecker JP, Logothetis NK. Different forms of effective connectivity in primate frontotemporal pathways Nat Commun. 2015; 6:6000.doi: 10.1038/ncomms7000 [PubMed: 25613079]

Powers AR, Hevey MA, Wallace MT. Neural Correlates of Multisensory Perceptual Learning J Neurosci. 2012; 32(18):6263–6274. DOI: 10.1523/Jneurosci.6138-11.2012 [PubMed: 22553032]

Rauschecker JP, Scott SK. Maps and streams in the auditory cortex: nonhuman primates illuminate human speech processing Nat Neurosci. 2009; 12(6):718–724. DOI: 10.1038/Nn.2331 [PubMed: 19471271]

Rauschecker JP, Tian B. Mechanisms and streams for processing of “what” and “where” in auditory cortex Proc Natl Acad Sci U S A. 2000; 97(22):11800–11806. DOI: 10.1073/pnas.97.22.11800 [PubMed: 11050212]

Redcay E. The superior temporal sulcus performs a common function for social and speech perception: Implications for the emergence of autism Neurosci Biobehav R. 2008; 32(1):123–142. DOI: 10.1016/J.Neubiorev.2007.06.004

Robinson JL, Laird AR, Glahn DC, Blangero J, Sanghera MK, Pessoa L, Fox PM, Uecker A, Friehs G, Young KA, Griffin JL, Lovallo WR, Fox PT. The functional connectivity of the human caudate: an application of meta-analytic connectivity modeling with behavioral filtering Neuroimage. 2012; 60(1):117–129. DOI: 10.1016/j.neuroimage.2011.12.010 [PubMed: 22197743]

Robinson JL, Laird AR, Glahn DC, Lovallo WR, Fox PT. Metaanalytic Connectivity Modeling: Delineating the Functional Connectivity of the Human Amygdala Hum Brain Mapp. 2010; 31(2):173–184. DOI: 10.1002/Hbm.20854 [PubMed: 19603407]

Rockland KS, Pandya DN. Cortical Connections of the Occipital Lobe in the Rhesus-Monkey - Interconnections between Areas 17, 18, 19 and the Superior Temporal Sulcus Brain Res. 1981; 212(2):249–270. DOI: 10.1016/0006-8993(81)90461-3 [PubMed: 7225868]

Romanski LM, Tian B, Fritz J, Mishkin M, Goldman-Rakic PS, Rauschecker JP. Dual streams of auditory afferents target multiple domains in the primate prefrontal cortex Nat Neurosci. 1999; 2(12):1131–1136. DOI: 10.1038/16056 [PubMed: 10570492]

Said CP, Moore CD, Engell AD, Todorov A, Haxby JV. Distributed representations of dynamic facial expressions in the superior temporal sulcus J Vision. 2010; 10(5)doi: 10.1167/10.5.11

Seltzer B, Pandya DN. Frontal-Lobe Connections of the Superior Temporal Sulcus in the Rhesus-Monkey J Comp Neurol. 1989; 281(1):97–113. DOI: 10.1002/Cne.902810108 [PubMed: 2925903]

Seltzer B, Pandya DN. Parietal, temporal, and occipital projections to cortex of the superior temporal sulcus in the rhesus monkey: a retrograde tracer study J Comp Neurol. 1994; 343(3):445–463. DOI: 10.1002/cne.903430308 [PubMed: 8027452]

Shattuck DW, Mirza M, Adisetiyo V, Hojatkashani C, Salamon G, Narr KL, Poldrack RA, Bilder RM, Toga AW. Construction of a 3D probabilistic atlas of human cortical structures Neuroimage. 2008; 39(3):1064–1080. DOI: 10.1016/j.neuroimage.2007.09.031 [PubMed: 18037310]

Shih P, Keehn B, Oram JK, Leyden KM, Keown CL, Muller RA. Functional Differentiation of Posterior Superior Temporal Sulcus in Autism: A Functional Connectivity Magnetic Resonance

Imaging Study Biol Psychiat. 2011; 70(3):270–277. DOI: 10.1016/J.Biopsych.2011.03.040 [PubMed: 21601832]

Simmons WK, Martin A. Spontaneous resting-state BOLD fluctuations reveal persistent domain-specific neural networks Soc Cogn Affect Neur. 2012; 7(4):467–475. DOI: 10.1093/Scan/Nsr018

Sokolov AA, Erb M, Gharabaghi A, Grodd W, Tatagiba MS, Pavlova MA. Biological motion processing: The left cerebellum communicates with the right superior temporal sulcus Neuroimage. 2012; 59(3):2824–2830. DOI: 10.1016/J.Neuroimage.2011.08.039 [PubMed: 22019860]

Sokolov AA, Erb M, Grodd W, Pavlova MA. Structural Loop Between the Cerebellum and the Superior Temporal Sulcus: Evidence from Diffusion Tensor Imaging Cereb Cortex. 2014; 24(3): 626–632. DOI: 10.1093/Cercor/Bhs346 [PubMed: 23169930]

Stevenson RA, James TW. Audiovisual integration in human superior temporal sulcus: Inverse effectiveness and the neural processing of speech and object recognition Neuroimage. 2009; 44(3): 1210–1223. DOI: 10.1016/J.Neuroimage.2008.09.034 [PubMed: 18973818]

Tian B, Reser D, Durham A, Kustov A, Rauschecker JP. Functional specialization in rhesus monkey auditory cortex Science. 2001; 292(5515):290–293. DOI: 10.1126/science.1058911 [PubMed: 11303104]

Turk-Browne NB, Norman-Haignere SV, McCarthy G. Face-specific resting functional connectivity between the fusiform gyrus and posterior superior temporal sulcus Front Hum Neurosci. 2010; 4doi: 10.3389/Fnhum.2010.00176

Turkeltaub PE, Eden GF, Jones KM, Zeffiro TA. Meta-analysis of the functional neuroanatomy of single-word reading: Method and validation Neuroimage. 2002; 16(3):765–780. DOI: 10.1006/Nimg.2002.1131 [PubMed: 12169260]

Turkeltaub PE, Eickhoff SB, Laird AR, Fox M, Wiener M, Fox P. Minimizing within-experiment and within-group effects in activation likelihood estimation meta-analyses Hum Brain Mapp. 2012; 33(1):1–13. DOI: 10.1002/Hbm.21186 [PubMed: 21305667]

Turken AU, Dronkers NF. The neural architecture of the language comprehension network: converging evidence from lesion and connectivity analyses Front Syst Neurosci. 2011; 5:1.doi: 10.3389/fnsys.2011.00001 [PubMed: 21347218]

Tzourio-Mazoyer N, Landeau B, Papathanassiou D, Crivello F, Etard O, Delcroix N, Mazoyer B, Joliot M. Automated anatomical labeling of activations in SPM using a macroscopic anatomical parcellation of the MNI MRI single-subject brain Neuroimage. 2002; 15(1):273–289. DOI: 10.1006/nimg.2001.0978 [PubMed: 11771995]

van Atteveldt N, Roebroeck A, Goebel R. Interaction of speech and script in human auditory cortex: Insights from neuro-imaging and effective connectivity Hearing Res. 2009; 258(1–2):152–164. DOI: 10.1016/J.Heares.2009.05.007

Warren JE, Wise RJ, Warren JD. Sounds do-able: auditory-motor transformations and the posterior temporal plane Trends Neurosci. 2005; 28(12):636–643. DOI: 10.1016/j.tins.2005.09.010 [PubMed: 16216346]

Yeterian EH, Pandya DN. Corticothalamic connections of the superior temporal sulcus in rhesus monkeys Exp Brain Res. 1991; 83(2):268–284. [PubMed: 2022239]

Zald DH, McHugo M, Ray KL, Glahn DC, Eickhoff SB, Laird AR. Meta-Analytic Connectivity Modeling Reveals Differential Functional Connectivity of the Medial and Lateral Orbitofrontal Cortex Cereb Cortex. 2014; 24(1):232–248. DOI: 10.1093/Cercor/Bhs308 [PubMed: 23042731]

Zhang H, Tian J, Liu JG, Li J, Lee K. Intrinsically organized network for face perception during the resting state Neurosci Lett. 2009; 454(1):1–5. DOI: 10.1016/J.Neulet.2009.02.054 [PubMed: 19429043]

Zilbovicius M, Meresse I, Chabane N, Brunelle F, Samson Y, Boddaert N. Autism, the superior temporal sulcus and social perception Trends Neurosci. 2006; 29(7):359–366. DOI: 10.1016/J.Tins.2006.06.004 [PubMed: 16806505]

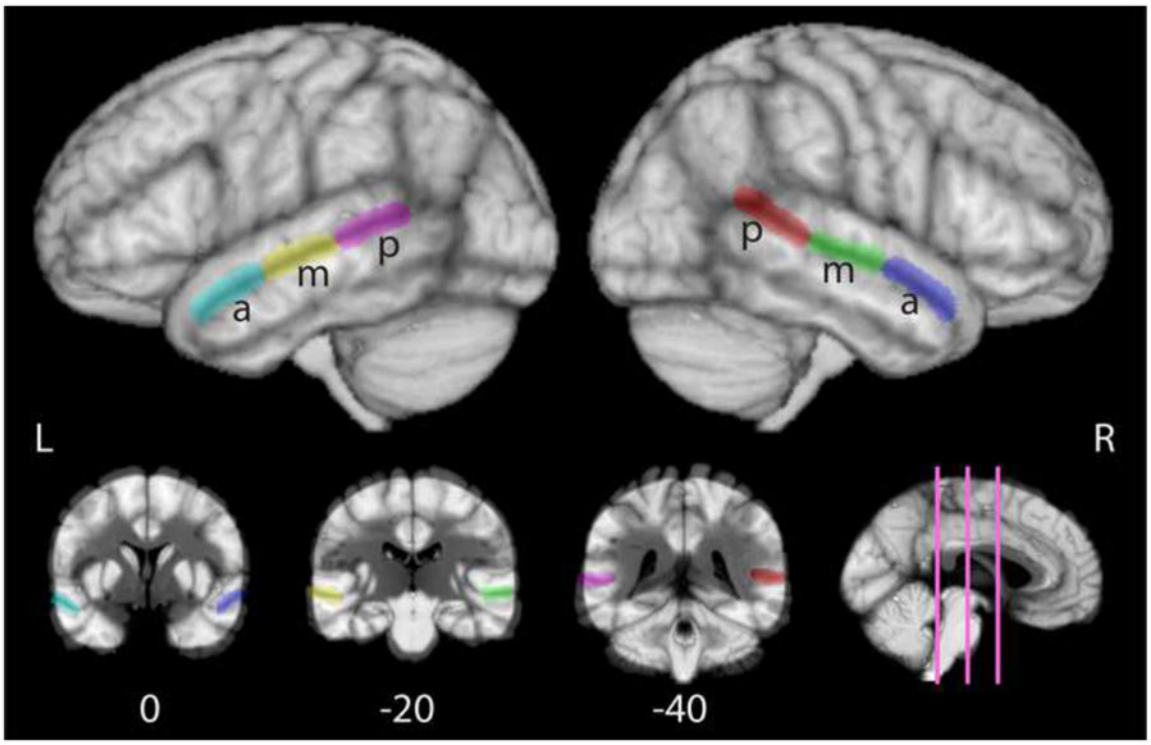

Fig.1. Six anatomical STS ROIs.

Six anatomical STS ROIs were manually created covering the anterior (a), middle (m), and posterior (p) subregions of the STS in each hemisphere, using the lpba140 max probabilistic atlas to estimate STS trajectory and location (see methods). Designations of a, m, and p subregions were estimated by proximity to Heschl's gyrus, where the LpSTS (purple) and RpSTS (red) were drawn just posterior to Heschl's gyrus, the LmSTS (yellow) and RmSTS (green) were drawn lateral to Heschl's gyrus, and the LaSTS (cyan) and RaSTS (blue) were drawn anterior to Heschl's gyrus. The STS ROIs are displayed on rendered hemispheres and coronal slices of the lpba40 max probabilistic atlas with the Colin27 template brain overlaid.

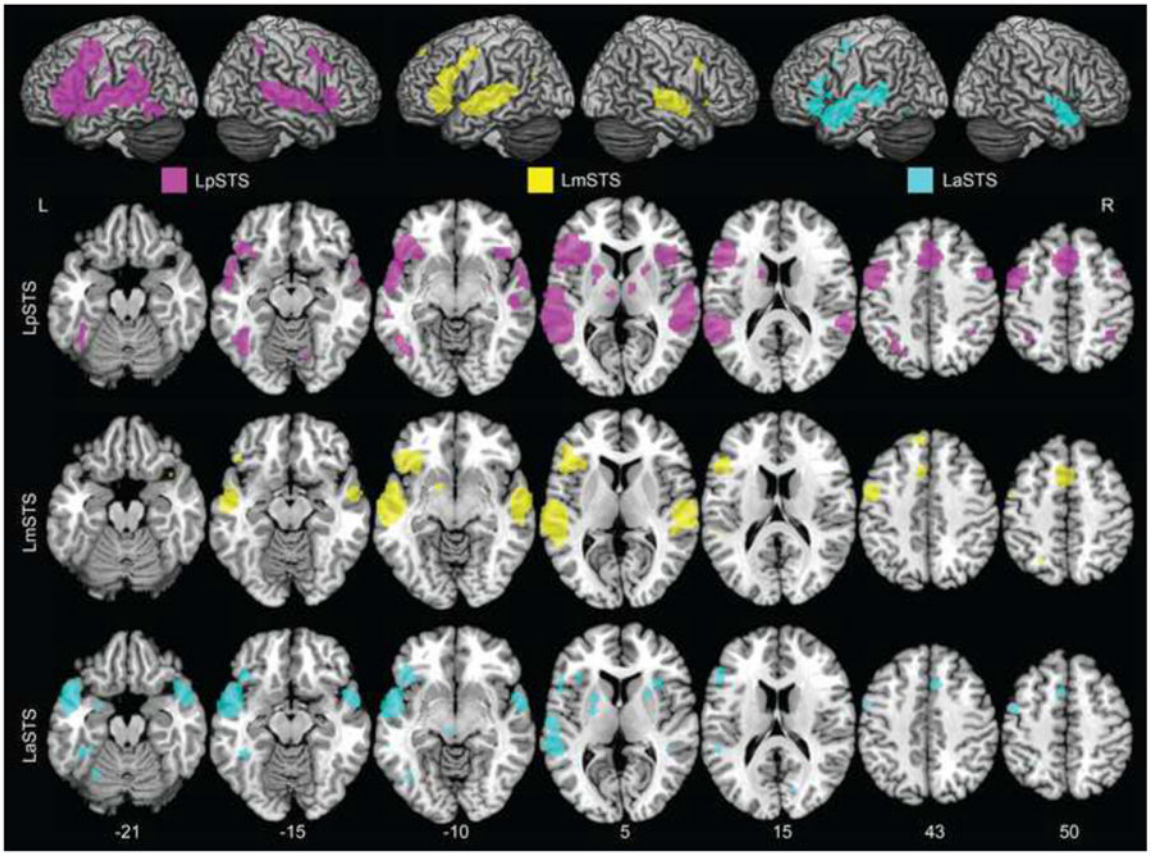

Fig.2. Left STS coactivation ALE results.

Consistent coactivation maps associated with the LpSTS (purple), LmSTS (yellow), and LaSTS (cyan) are displayed. ALE analyses were conducted on each set of experiments to evaluate the brain regions that were consistently coactivated with different left STS subregions. All ALE results are reported with an FDR of 0.001 and cluster threshold of 100 mm^3. Number of experiments identified are listed in Table 1.

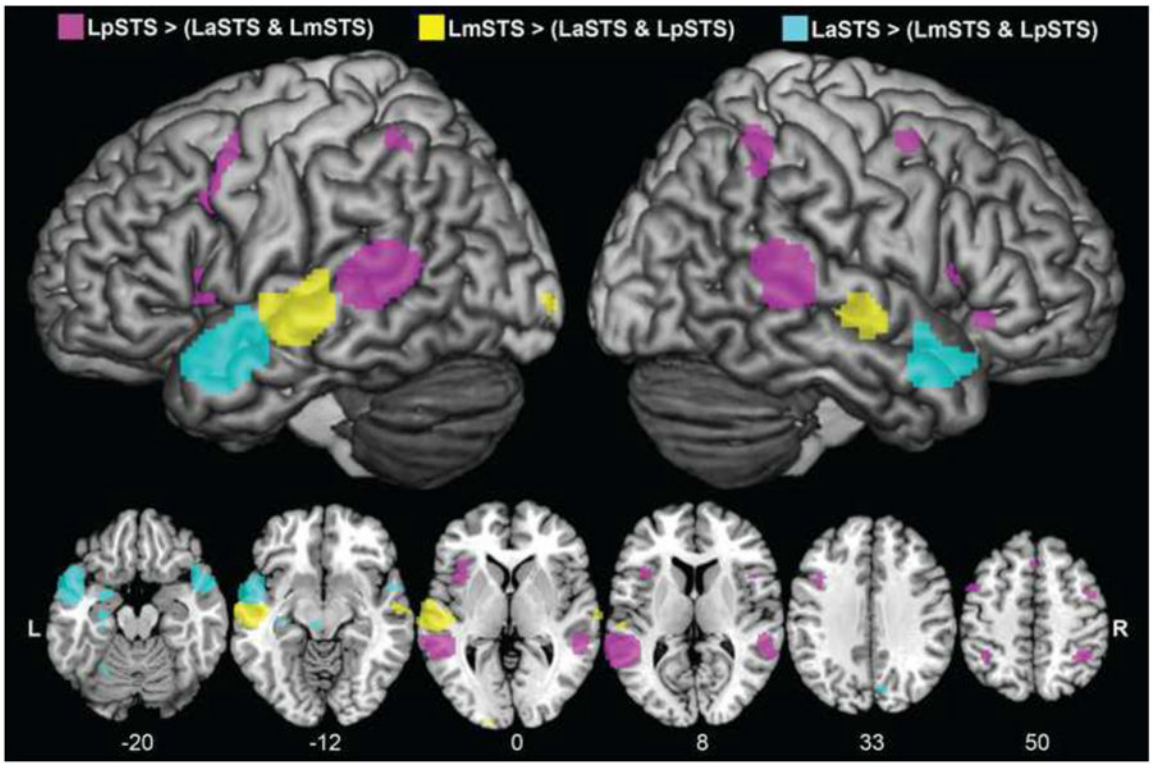

Fig.3. Left STS subtraction ALE results.

Coactivation maps for the left STS subregions were directly compared through ALE subtraction analyses (see Table 4). The LpSTS (purple) as compared to the LaSTS and LmSTS had more coactivation in auditory and language dorsal-stream regions, such as bilateral IPL. The LaSTS (cyan) as compared to the LmSTS and LpSTS had more coactivation in some auditory and language ventral-stream regions, such as the right STG/MTG pole. The LmSTS (yellow) as compared to the LaSTS and LpSTS had more coactivation in the right middle STS and left calcarine cortex (VI). The subtraction ALE analyses were conducted with 10,000 permutations, an FDR of 0.05 and a cluster threshold of 100 mm^3.

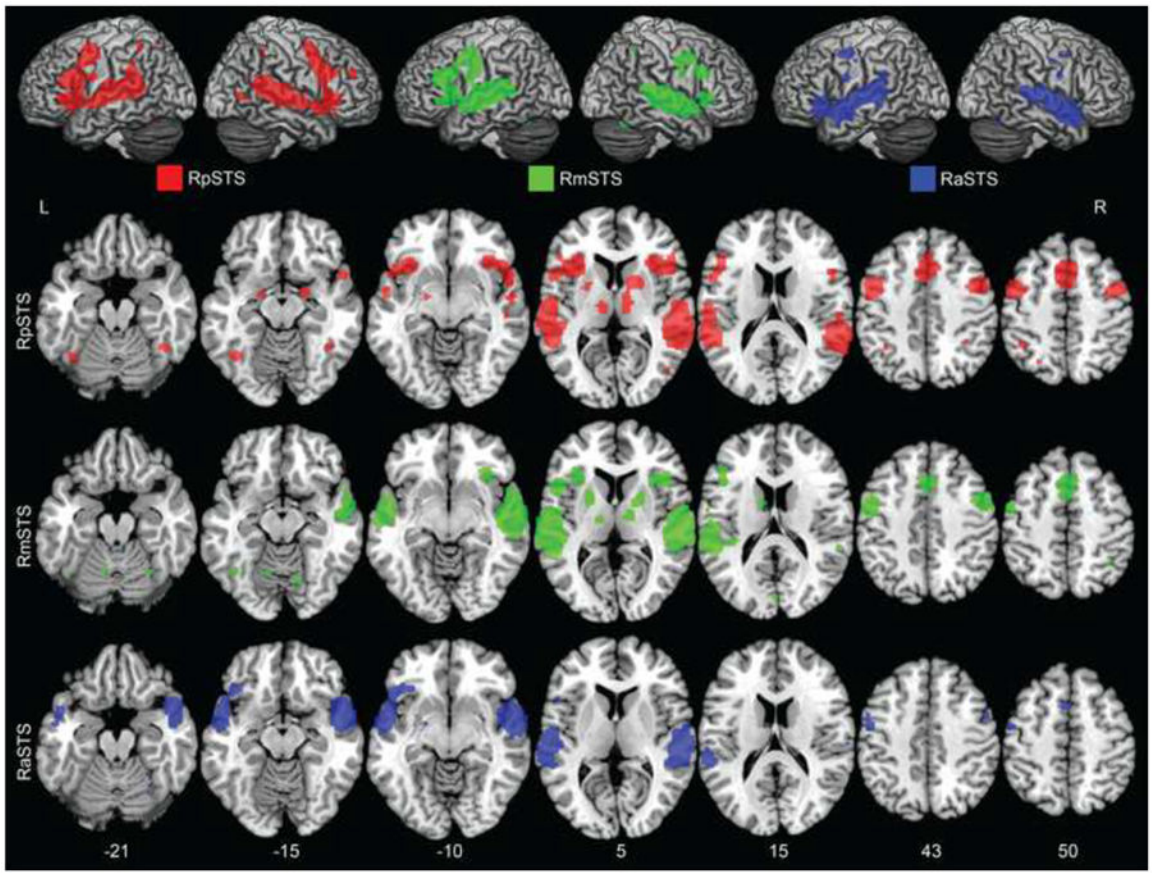

Fig.4. Right STS coactivation ALE results.

Consistent coactivation maps across experiments for the RpSTS (red), RmSTS (green), and RaSTS (blue) were identified. The ALE results are reported as in Figure 2; and number of experiments identified are listed in Table 1.

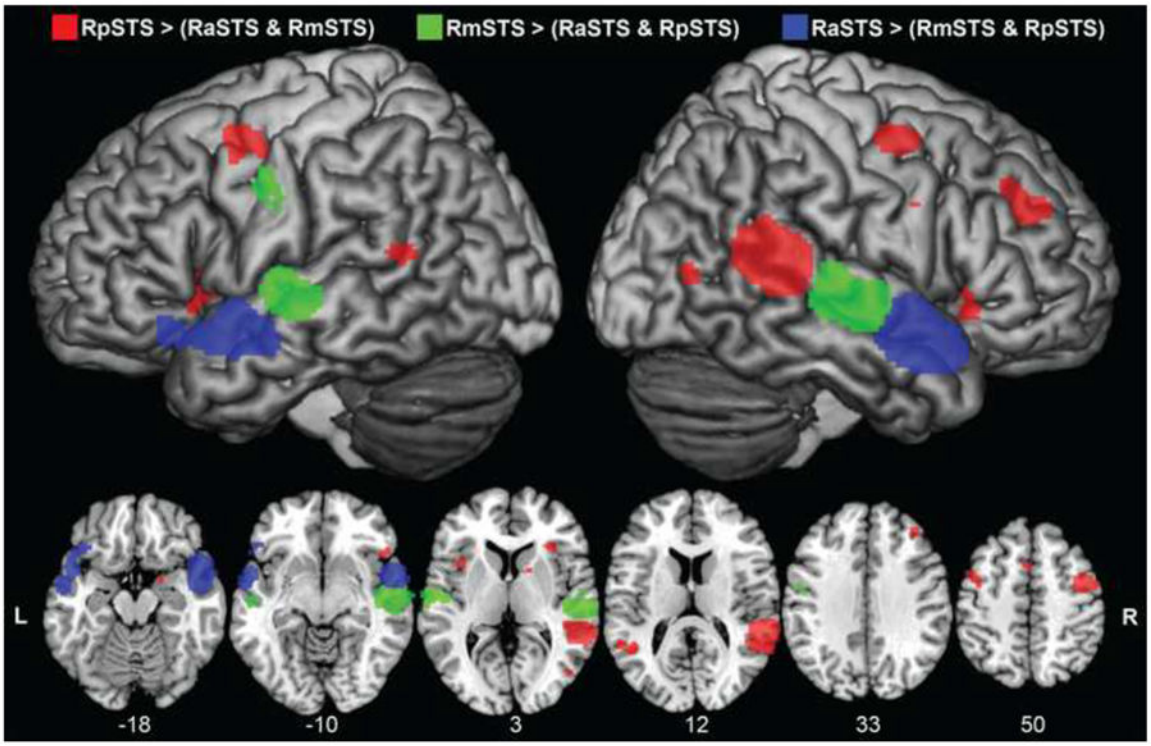

Fig.5. Right STS subtraction ALE results.

Direct comparisons of the right STS subregion coactivation maps are presented (see Table 5). The RpSTS (red) compared to the RaSTS and RmSTS had more coactivation in auditory and language dorsal-stream regions, such as bilateral precentral gyrus. The RaSTS (blue) compared to the RmSTS and RpSTS had more coactivation in auditory and language ventral-stream regions, including ALE peaks in the left anterior MTG and left IFG pars orbitalis. The RmSTS (green) compared to the RaSTS and RpSTS had more coactivation in left Heschl's gyrus and left MTG. The subtraction ALE results are reported as in Figure 3.

Table 1.

The BrainMap functional database search results identified for each STS ROI.

Several experiments reported foci in more than one ROI. The number in parentheses represents the number of experiments in each ROI that did not report activations in another STS ROI in the same hemisphere. The totals designated by an asterisk reflect the number of unique experiments across all ROIs in that hemisphere, where experiments were only counted once even if the experiments reported activations in more than one STS ROI in the same hemisphere. Thus, the cumulative totals reported do not match the overall sum of experiments across ROIs.

STS ROI	Papers	Subjects	Experiments	Foci
LaSTS	65	1014	78 (49)	1339
LmSTS	131	1794	161 (124)	2156
LpSTS	182	2767	255 (206)	3906
RaSTS	76	1034	92 (60)	1464
RmSTS	133	1893	192 (147)	2906
RpSTS	167	2616	215 (169)	3495
Left STS Total*		6071*	434*	6415*
Right STS Total*		6021*	435*	6659*

Table 2.

BrainMap behavioral classifications of experiments identified for each left STS ROI.

For the left STS ROIs, this table provides “raw counts” of experiments for each BrainMap behavioral classification and the “ROI proportion relative to BrainMap” which is the comparison of experiments classified per behavioral category in each ROI and the BrainMap database. For “ROI proportion relative to BrainMap” results, behavioral categories with values greater than 1 had a larger proportion of experiments classified as that behavior in the ROI as compared to the BrainMap database. Chi square analyses were also conducted .

	raw counts				ROI proportion relative to BrainMap		
Behavioral Category	**laSTS**	**lmSTS**	**IpSTS**	**BrainMap**	**laSTS**	**lmSTS**	**IpSTS**
Action.Execution.Other	0	5	10	952	0	0.37	0.46
Action.Execution.Speech	3	7	18	342	1.26	1.43	2.32**
Action.Imagination	0	2	2	129	0	1.08	0.68
Action.Inhibition	1	8	10	379	0.38	1.47	1.16
Action.Motor Learning	1	1	1	93	1.55	0.75	0.47
Action.Observation	0	3	6	122	0	1.72	2.17
Action.Preparation	0	0	0	50	0	0	0
Action.Rest	0	0	0	267	0	0	0
Cognition.Attention	6	17	33	1561	0.55	0.76	0.93
Cognition.Language.Orthography	0	9	7	231	0	2.72*	1.33
Cognition.Language.Other	5	3	3	168	4.29*	1.25	0.79
Cognition.Language.Phonology	3	15	12	236	1.83	4.43**	2.24*
Cognition.Language.Semantics	19	31	77	1125	2.43**	1.92**	3.02**
Cognition.Language.Speech	15	29	69	915	2.36**	2.21**	3.32**
Cognition.Language.Syntax	1	5	6	120	1.20	2.91	2.20
Co gnition.Memory.Explicit	6	10	15	927	0.93	0.75	0.71
Co gnition.Memory.Other	0	1	0	52	0	1.34	0
Co gnition.Memory.Working	1	11	14	954	0.15	0.80	0.65
Cognition.Music	0	2	4	100	0	1.40	1.76
Cognition.Other	11	12	11	1143	1.39	0.73	0.42*
Cognition.Reasoning	0	3	2	218	0	0.96	0.40
Cognition.Social Cognition	1	7	13	252	0.57	1.94	2.27*
Cognition.Soma	1	0	0	89	1.62	0	0
Cognition.Space	1	2	1	215	0.67	0.65	0.20
Cognition.Time	1	1	2	61	2.36	1.14	1.44
Emotion.Anger	3	1	4	81	5.33*	0.86	2.18
Emotion.Anxiety	0	0	0	91	0	0	0
Emotion.Disgust	2	0	4	142	2.03	0	1.24
Emotion.Fear	2	1	3	253	1.14	0.28	0.52

	raw counts				ROI proportion relative to BrainMap		
Behavioral Category	**laSTS**	**lmSTS**	**lpSTS**	**BrainMap**	**laSTS**	**lmSTS**	**lpSTS**
Emotion.Happiness.Humor	0	0	0	23	0	0	0
Emotion.Happiness.Other	5	1	1	191	3.77*	0.37	0.23
Emotion.Other	15	25	28	1922	1.12	0.91	0.64
Emotion.Sadness	3	2	0	193	2.24	0.72	0
Interoception.Air-Hunger	0	0	0	17	0	0	0
Interoception.Bladder	0	0	0	42	0	0	0
Interoception.Hunger	1	0	0	66	2.18	0	0
Interoception.Other	0	0	3	27	0	0	4.89
Interoception.Sexuality	0	0	1	111	0	0	0.40
Interoception.Sleep	0	1	0	43	0	1.62	0
Interoception.Thermoregulation	0	0	0	3	0	0	0
Interoception.Thirst	0	0	0	24	0	0	0
Perception.Audition	12	27	22	426	4.06**	4.42**	2.27**
Perception.Gustation	3	1	3	191	2.26	0.37	0.69
Perception.Olfaction	0	1	0	86	0	0.81	0
Perception.Somethesis.Other	2	1	7	436	0.66	0.16	0.71
Perception.Somethesis.Pain	2	1	1	366	0.79	0.19	0.12
Perception.Vision.Color	0	0	0	22	0	0	0
Perception.Vision.Motion	1	2	2	269	0.54	0.52	0.33
Perception.Vision.Other	1	3	9	308	0.47	0.68	1.29
Perception.Vision.Shape	1	2	6	467	0.31	0.30	0.57
Total experiments identified	**78**	**161**	**255**	**11233**			

*($p < 0.01$ and

**$p < 0.001$)

Table 3.

BrainMap behavioral classifications of experiments identified for each right STS ROI.

Same information as described in Table 2, except data represent the right STS ROIs.

	raw counts				ROI proportion relative to BrainMap		
Behavioral Category	**raSTS**	**rmSTS**	**rpSTS**	**BrainMap**	**raSTS**	**rmSTS**	**rpSTS**
Action.Execution. Other	3	5	11	952	0.38	0.31*	0.60
Actio n.Execution. Speech	5	19	10	342	1.79	3.25**	1.53
Action. Imagination	0	1	0	129	0	0.45	0
Action. Inhibition	2	10	10	379	0.64	1.54	1.38
Action.Motor Learning	0	0	0	93	0	0	0
Action. Observation	2	3	7	122	2.00	1.44	3.00*
Action.Preparation	0	0	0	50	0	0	0
Action.Rest	0	0	0	267	0	0	0
Cognition. Attention	13	25	42	1561	1.02	0.94	1.41
Cognition.Language.Orthography	1	4	3	231	0.53	1.01	0.68
Cognition.Language.Other	1	5	2	168	0.73	1.74	0.62
Cognition.Language.Phonology	6	6	7	236	3.10*	1.49	1.55
Cognition.Language.Semantics	17	39	40	1125	1.85	2.03**	1.86**
Cognition. Language. Speech	21	40	47	915	2.80**	2.56**	2.68**
CognitiomLanguage. Syntax	1	3	3	120	1.02	1.46	1.31
Cognition.Memory.Explicit	5	11	10	927	0.66	0.69	0.56
Cognition.Memory.Other	1	1	3	52	2.35	1.13	3.01
Cognition.Memory. Working	2	7	10	954	0.26	0.43	0.55
CognitionMusic	5	8	8	100	6.10**	4.68**	4.18**
Cognition. Other	8	14	10	1143	0.85	0.72	0.46*
Cognition.Reasoning	0	3	5	218	0	0.81	1.20
Cognition. Social Cognition	3	3	7	252	1.45	0.70	1.45
Cognition. Soma	0	2	0	89	0	1.31	0
Cognition. Space	0	1	2	215	0	0.27	0.49
Cognition.Time	0	2	4	61	0	1.92	3.43
Emotion. Anger	2	0	3	81	3.01	0	1.94
Emotion. Anxiety	0	0	0	91	0	0	0
EmotiomDisgust	1	0	3	142	0.86	0	1.10
Emotion.Fear	1	2	9	253	0.48	0.46	1.86
Emotion.Happiness.Humor	0	0	0	23	0	0	0
Emotion.Happiness.Other	1	3	2	191	0.64	0.92	0.55
Emotion. Other	20	23	34	1922	1.27	0.70	0.92
Emotion. Sadness	1	1	3	193	0.63	0.30	0.81
Interoception. Air-Hunger	0	0	0	17	0	0	0
InteroceptiomBladder	0	1	0	42	0	1.39	0

	raw counts				ROI proportion relative to BrainMap		
Behavioral Category	**raSTS**	**rmSTS**	**rpSTS**	**BrainMap**	**raSTS**	**rmSTS**	**rpSTS**
Interoception.Hunger	0	0	1	66	0	0	0.79
Interoception. Other	0	3	0	27	0	6.50*	0
Interoception. Sexuality	0	2	2	111	0	1.05	0.94
Interoception. Sleep	0	1	0	43	0	1.36	0
Interoception. Thermoregulation	0	0	0	3	0	0	0
Interoception. Thirst	0	0	0	24	0	0	0
Perception. Audition	22	40	24	426	6.31**	5.49**	2.94**
Perception. Gustation	1	0	1	191	0.64	0	0.27
Perception. Olfaction	0	2	1	86	0	1.36	0.61
Perception. Somethesis.Other	0	5	5	436	0	0.67	0.60
Perception. Somethesis.Pain	1	0	2	366	0.33	0	0.29
Perception. Vision. Color	0	0	0	22	0	0	0
Perception. Vision.Motion	0	0	5	269	0	0	0.97
Perception. Vision. Other	2	9	8	308	0.79	1.71	1.36
Perception. Vision. Shape	2	3	6	467	0.52	0.38	0.67
Total experiments identified	**92**	**192**	**215**	**11233**			

Table 4.

Left STS subtraction ALE results.

The ALE results are reported with an FDR of 0.05 and cluster threshold of 100 mm^3. The first cluster listed for each subtraction represents the co-localization of foci identified from the searched ROI.

Brain Region	Volume (mm^3)	Z value	MNI		
			x	y	Z
LpSTS > (LaSTS & LmSTS)					
1) L MTG	10832	3.89	−56	−45	7
2) R MTG	4272	3.89	56	−42	5
3) R IPL	1640	3.89	37	−50	51
4) L Insula	1528	3.89	−37	12	3
5) L Precentral Gyrus	1336	3.54	−41	10	32
L Precentral Gyrus		3.24	−42	8	42
L Precentral Gyrus		3.16	−42	4	48
L Precentral Gyrus		3.01	−48	4	46
L Precentral Gyrus		2.99	−48	4	52
6) L IPL	520	3.35	−38	−50	52
LIPL		3.24	−36	−48	48
7) L SMA	376	3.12	2	22	49
R Medial SFG		2.95	6	26	46
8) R MFG	352	3.89	46	0	53
9) R IFG - Orbitalis	288	3.43	56	24	−8
RIFG - Orbitalis		3.35	52	24	−8
10) R IFG - Opercularis	152	3.04	46	12	8
LmSTS > (LaSTS & LpSTS)					
1) L MTG	9960	3.89	−59	−19	−6
2) R STS	2224	3.89	61	−14	−8
R STS		3.72	70	−17	−4
3) L Calcarine / Mid. Occipital Lobe	168	3.19	−16	−104	−2
LaSTS > (LmSTS & LpSTS)					
1) L MTG	9408	3.89	−53	4	−18
2) R MTG Pole	3832	3.89	53	8	−23
R MTG Pole		3.72	50	10	−28
3) L Hippocampus	1872	3.89	−28	−14	−20
L Hippocampus		3.04	−30	−24	−12
4) L Midbrain	248	3.19	−5	−25	−12
5) L Cerebellum	120	3.35	−25	−61	−18
6) R Cuneus	112	3.19	10	−77	33

Abbreviations: L = left hemisphere; R = right hemisphere; SFG = superior frontal gyrus.

Table 5.

Right STS subtraction ALE results.

The ALE results are reported with an FDR of 0.05 and cluster threshold of 100 mm^3. The first cluster for each subtraction result represents the co-localization of foci identified from the searched ROI. Abbreviations match Table 4.

Brain Region	Volume (mm^3)	Z value	MNI		
			X	y	Z
RpSTS > (RaSTS & RmSTS)					
1) RMTG	11120	3.89	58	−44	9
2) R Precentral Gyrus	2000	3.89	42	−4	49
3) R Insula	1400	3.89	32	27	7
RIFG - Orbitalis		3.29	47	20	−6
RIFG - Opercularis		3.19	52	20	−2
R Insula		2.97	40	22	−6
4) L Precentral Gyrus	1088	3.89	−41	0	49
L Precentral Gyrus		3.43	−48	6	52
5) RMFG	984	3.89	32	39	27
RMFG		3.54	32	46	26
6) L MTG	696	3.43	−47	−54	12
LMTG		3.35	−48	−52	13
7) L Insula	688	3.54	−36	10	4
L Insula		3.29	−38	12	0
L Insula		2.99	−36	16	−6
8) L SMA	432	3.12	−4	8	54
L SMA		3.09	1	10	52
9) R MTG	288	3.29	48	−72	5
10) R Globus Pallidus	184	3.19	16	6	2
11)R Amygdala	112	3.06	22	0	−18
12) R IFG - Opercularis	112	2.99	40	2	27
R Precentral Gyrus		2.81	48	4	28
RmSTS > (RaSTS & RpSTS)					
1) R STS	11248	3.89	56	−19	−4
2) L MTG	4216	3.89	−58	−17	−3
LMTG		3.72	−52	−15	−6
L Heschl's Gyrus		3.09	−46	−12	4
3) L Precentral Gyrus	520	3.19	−54	−5	35
L Postcentral Gyrus		2.97	−46	−12	30
RaSTS > (RmSTS & RpSTS)					
1) RMTG Pole	10512	3.89	53	5	−16
2) L MTG	6376	3.89	−57	−1	−14
L IFG - Orbitalis		3.54	−41	24	−15